ACS APPLIED MATERIALS & INTERFACES

Research Article

www.acsami.org

High-Performance Light-Emitting Diodes Encapsulated with Silica-Filled Epoxy Materials

Tian Li, Jie Zhang, Huiping Wang, Zhongnan Hu, and Yingfeng Yu*

State Key Laboratory of Molecular Engineering of Polymers, Department of Macromolecular Science, Fudan University, Shanghai 200433, China

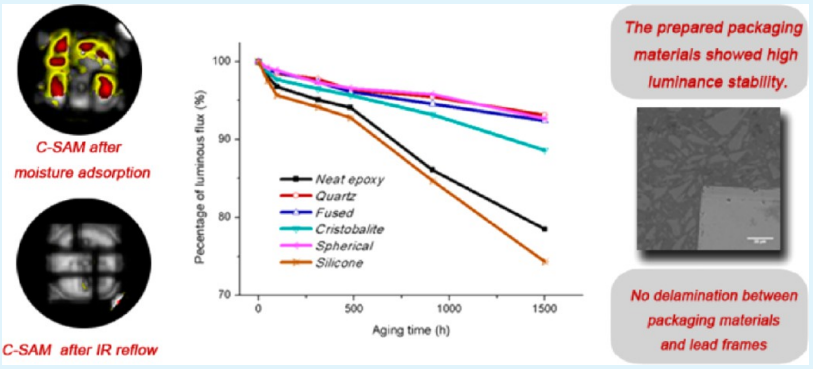

ABSTRACT: Packaging materials have a great impact on the performance and reliability of light-emitting diodes (LEDs). In this study, we have prepared high performance LED devices through encapsulating LEDs by epoxy materials incorporated with filler powders. A set of evaluation methods have also been established to characterize the reliability of LED devices. No delamination or internal cracking between packaging materials and lead frames has been found for the encapsulated high performance LED devices after the package saturation with moisture and subsequent exposure to high-temperature solder reflow and thermal cycling. Four kinds of inorganic silica fillers, namely, quartz, fused silica, cristobalite, and spherical silica, and one kind of organic filler, that is, spherical silicone powder, were incorporated into the epoxy packaging materials to compare their effects on performance of LED devices. The properties of epoxy packaging materials and LED devices were studied by differential scanning calorimetry (DSC), thermogravimetric analyses (TGA), dynamic mechanical analysis (DMA), thermomechanical analyzer (TMA), ultravioletvisible spectrophotometer (UV−vis), scanning acoustic microscopy (SAM), and scanning electron microscopy (SEM). Except the spherical silicone powder filled epoxy materials, all the other filled systems showed lower equilibrium water sorption content and smaller water diffusion coefficient in both water sorption and moisture sorption tests. The coefficient of thermal expansion (CTE) values were also decreased with the addition of fillers, and the systems filled with quartz, fused, and filled with spherical silica gave the best performance, which exhibited the reduced CTE values both below and above T_g. The results of TGA essentially showed no difference between filled and unfilled systems. The glass transition temperature changed little for all the filled systems, except the one incorporated with spherical silicone. The modulus at room temperature increased with the addition of fillers. The light transmittance of filled epoxy materials varied with fillers after UV and thermal aging.

KEYWORDS: *light-emitting diodes, epoxy packaging materials, fillers, device reliability*

1. INTRODUCTION

In recent years, light-emitting diodes (LEDs) have been widely applied in many areas, including displaying, lighting, communications, medical services, signage, and general illuminations.[1−3] Compared with the rapid advances in LED chips, the performance of LED devices, especially their reliability, needs much improvement due to the packaging materials and reliability test methods developing a bottleneck.[4]

Surface mount technology is used extensively to mount the LED packages for practical application. For display applications, surface-mounted devices (SMDs) provide much higher resolution than former duel-inline packaged lamp type LEDs. From the point of view of mechanical and optical properties, epoxy-based materials provide a quite balanced performance for SMD packaging. With their unique chemical and physical properties such as excellent chemical and corrosion resistances, electrical and physical properties, excellent adhesion, thermal insulation, low shrinkage, and reasonable material cost, epoxy materials have been most widely employed for display packaging.[4−10]

However, during the surface mount reflow soldering process, both the device body and leads are intentionally heated to temperature as high as 240−260 °C, which results in a buildup of stresses within the devices due to rapid vaporization of absorbed moisture, coefficient of thermal expansion (CTE) mismatches at

Received: May 28, 2013
Accepted: August 26, 2013
Published: August 26, 2013

the internal interfaces, and decrease in the adhesive strength of the epoxy packaging materials at high temperatures.[11−14] Delamination occurs when the total hygrothermal stress developed during solder reflow exceeds the adhesion strength of the interface and thus decreases the protective capacity of the packaging materials.[8,15−17]

In addition, the cold-heating thermal cycling as well as moisture sorption during LED devices exposed to harsh environments also cause internal stresses. Usually, epoxy materials have a typical CTE value in the range of 60−80 × 10^{-6}/K, while metals and ceramics have CTEs of about 10 × 10^{-6}/K; therefore, a minimum change of temperature might lead to important deformation differences between the different materials. The internal stresses thus generated at the bonded surfaces can result in the fatigue of wire ball bond and solder joint as well as delaminating problems between the LED die and packaging materials.[1,18] Consequently, failures of devices take place due to wires cracking or ionic corrosion through the delaminated surface.

In traditional microelectronic packaging techniques, including the epoxy molding compound, many efforts have been devoted to lower the internal stress of packaging materials, increase the interfacial bonding strength between packaging materials and metals or chips, and reduce the mismatch of CTE under cold or hot conditions.[19,20]

For crack-resistant low stress packaging materials, epoxy resins were selected to possess biphenyl and dicyclopentadiene structure[21−23] and modified with liquid rubber, like siloxane,[24] or core−shell rubber particles,[25] which can decrease the internal stress significantly but without sacrificing thermal properties due to the formation of double-phase structure.[26] In another aspect, adhesion promoters, such as organosilanes,[27] titanate,[28] and thiols,[29] etc., have also been widely applied to improve the interfacial interaction between the metal frame and packaging materials, while inorganic fillers, mostly silicas,[30,31] have been extensively incorporated to lower the CTE of packaging materials. There are also some reports on the loading of nanoparticles with high refractive index to improve the light output of the LED devices,[32,33] but their effects on the reliability need further study.

Nevertheless, the requirement of high light transmission with long-time stability of LED packaging materials limits the application of the above-mentioned methods. Epoxy materials with excellent weather resistance and high glass transition temperature can minimize the aging caused by sunlight and heating, as UV-light and thermal stability are required for outdoor and severe environment applications. Therefore, for LED packaging materials, numerous works have tried to improve the performance of packaging materials by introducing phenolic resin,[34] aromatic epoxy with bulk substitutions,[35] silicone segments,[36] etc., into epoxy resins with aliphatic structure.[7,37,38] However, none of these methods can relieve the mismatch of CTE between packaging materials and LED devices.

In this work, different kinds of fillers were incorporated into epoxy packaging materials with the expectation of reducing moisture and the thermal expansion mismatch between the packaging materials and the packaged parts. The fillers we chose are all in micrometer size because using fillers larger than micrometer scale would have a problem of filler sedimentation during storage and processing, while nanoscaled fillers would increase the viscosity of packaging materials sharply and thus make the fluid dispensing process unenforceable. By comparison of the performances of the micrometer-size fillers filled and unfilled epoxy materials, a silica-filled material with balanced properties has been found for the packaging of LEDs. In addition, a set of characterization methods have been established for the reliability and performance tests of LED packaging materials.

2. EXPERIMENTAL SECTION

2.1. Materials and Samples Preparation. All epoxies and anhydrides for the epoxy packaging materials were provide by Japan Companies, and the refractive index of the epoxy resin is about 1.49. According to the nondisclosure agreements with collaborative companies, the detailed components and preparation procedures of the materials are not listed here.

Five kinds of fillers with an average diameter of 5 μm and high purity (>99.9%), namely, quartz (crystal silica, purity >99.99%), fused silica, cristobalite, spherical silica, and spherical silicone powder (polymethylsilsesquioxane), were provided by Lianyungang Donghai Silica Powder Co. Ltd. (Lianyungang City, China) and used without further treatments. The refractive index and CTE of the fillers are listed in Table 1.

Table 1. Refractive Index and Coefficient of Thermal Expansion of Fillers

filler	quartz	fused silica	cristobalite	spherical silica	silicone powder
refractive index	1.54	1.458	1.50	1.458	1.42
coefficient of thermal expansion (ppm/°C)	11.2	0.55	54	0.55	--

As the surface-treating agents have been incorporated into the epoxy resin, the fillers were blended with epoxy directly under vacuum for 15 min by a centrifugal mixer, which has a revolution speed of 600 rpm, rotation speed of 350 rpm, and mixing angle of 45° oblique. The dispersion of fillers was tested by using the scraper fineness test. The weight ratio of filler to epoxy resin was selected as 40:60 in this study for all the filler-added materials as a balanced property was achieved at this proportion.

The six epoxy packaging materials are denoted as *neat epoxy, quartz, fused, cristobalite, spherical,* and *silicone*, on the basis of their composition and the added filler type. For example, *fused* means the fused silica added system, while *silicone* means the spherical silicone powder added system. The RGB type LEDs with the same chip and package structure were encapsulated with the epoxy materials and cured with the same procedure of 130 °C for 2 h and 150 °C for 4 h.

2.1.1. Moisture Preconditioning. The most severe industry test conditions, moisture/reflow sensitive level 1 test based on IPC/JEDEC J-STD-020, have been employed on the LED devices. The preconditioning procedures are as follows: the samples were first baked at 125 °C for 16 h to eliminate the residual moisture in the packaging materials; then suffered five rounds of −65 to 150 °C thermal cycling to simulate transporting from different sites; they were put into a chamber with 85 °C and 85% RH environment for 168 h. After cooling to room temperature at 100% relative humidity, the samples were subjected to infrared (IR) reflow three times with 260 °C peak temperature.

2.1.2. Thermal Shock Cycling Test. The thermal cycling (T/C) test after preconditioning was carried out by the following procedure:[16] a cycle consisted of −65 °C × 15 min and 150 °C × 15 min. The failure percentage and luminance of the LED devices were inspected after different test conditions.

2.1.3. Pressure Cooker Test (PCT). The PCT is a parallel experiment to the T/C test. Samples after moisture preconditioning were soaked in a PCT cell at 121 °C/100% RH/2 atm for 168 h.

2.2. Characterization. *2.2.1. Differential Scanning Calorimetry (DSC).* A TA Q2000 DSC instrument was used for the study of the curing reaction and the glass transition at a heating of 10 °C/min. Samples of approximately 5−10 mg in weight were cured in aluminum pans in a nitrogen atmosphere. The calorimeter was calibrated using

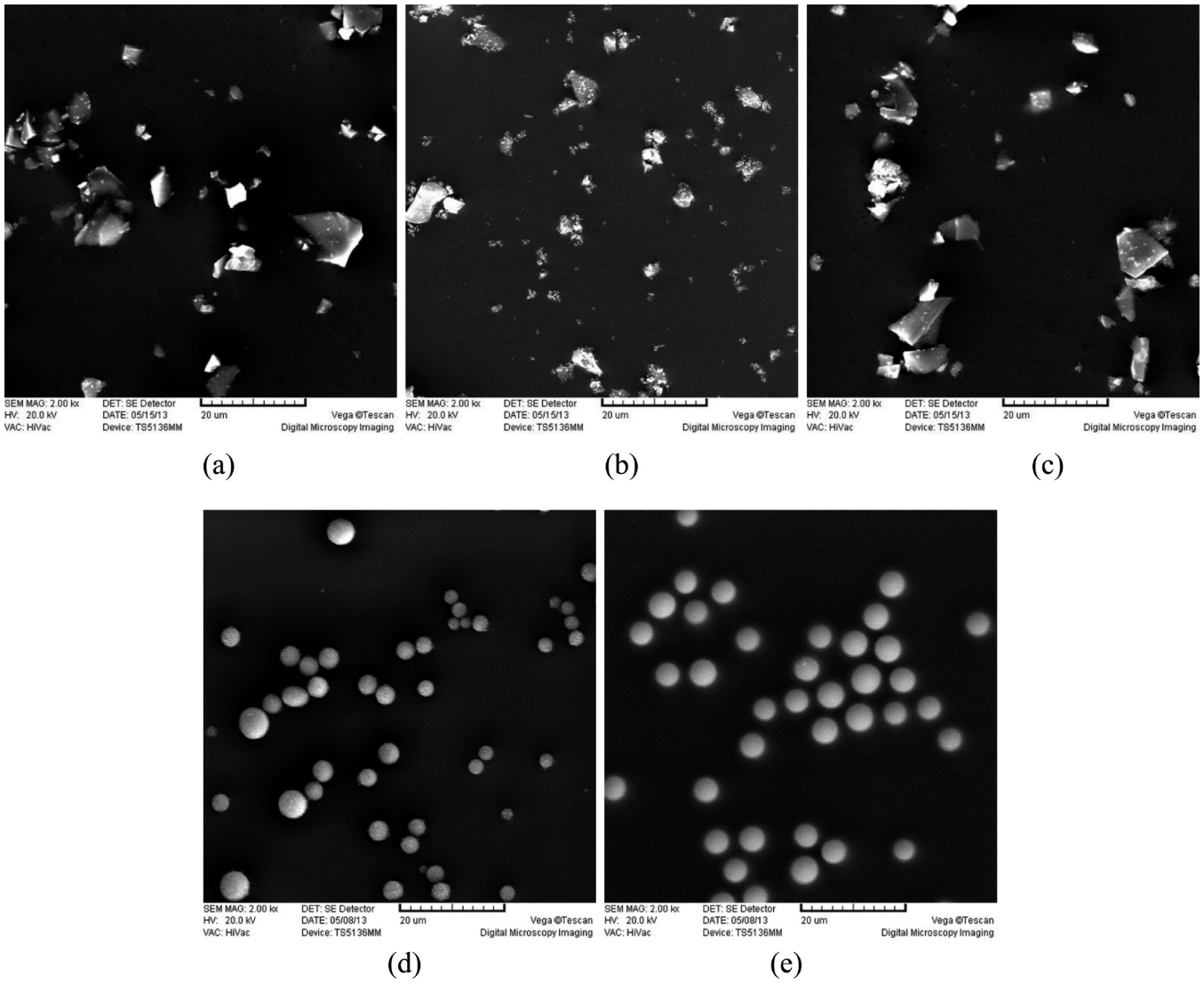

Figure 1. SEM micrographs for the morphologies of the five kinds of fillers: (a) quartz; (b) fused silica; (c) cristobalite; (d) spherical silica; (e) spherical silicone powder.

indium standard (heat flow calibration) and an indium−lead−zinc standard (temperature calibration).

2.2.2. Dynamic Mechanical Analysis (DMA). The dynamic mechanical properties were collected with a Netzsch DMA 242 operating in the single cantilever mode at an oscillation frequency of 1 Hz. The specimens for DMA were prepared in the form of bars with a nominal dimension of $2 \times 8 \times 20$ mm^3, and the data were collected from 50 to 260 °C at a scanning rate of 3 °C/min.

2.2.3. Thermogravimetric Analyses (TGA). Thermal decompositions were performed from room temperature to 800 °C on powdered samples with masses between 8 and 15 mg using a Perkin-Elmer Pyris1 TGA at a heating rate of 10 °C/min in a nitrogen atmosphere.

2.2.4. Thermomechanical Analyzer (TMA). The thermal expansion coefficients (CTEs, α) of the materials were measured using a Mettler Toledo SDTA841e TMA. The measurements were performed with the compression mode. The temperature range was from 50 to 270 °C, and the heating rate was 5 °C/min. CTEs were calculated according to the following equation from reading off the sample length with temperature change

$$a = \frac{dL}{dT} \times \frac{1}{L_T} \quad (1)$$

where dL/dT is the slope of the tangent on the sample length−temperature curve, and L_T is the sample length at T (°C).

2.2.5. Hardness Test. The hardness was measured at room temperature using a Shore D hardness tester (XHS, China) according to ASTM standard D2240.

2.2.6. Scanning Acoustic Microscopy (SAM). The C-mode scanning acoustic microscope (C-SAM) was used for monitoring interfacial delamination and package cracking by exposure to IR solder reflow. A C-SAM scan was performed using a SONIX system L/HF 200 equipped with a 15 MHz, 0.5" focal length transducer after each preconditioning step. This test utilizes a pulse-echo technique in which a high-frequency acoustic beam is focused on the interface within an IC package. The reflected acoustic wave coming from the interface is analyzed to determine if delamination or other defects are present. It semi-quantitatively gauges adhesion strength based on the degree of delamination without destroying the package.

2.2.7. Scanning Electron Microscope (SEM). The morphologies of fillers and filled epoxies were observed under a scanning electron microscope (TESCAN, TS 5136MM). All samples were coated with gold and mounted on copper mounts.

2.2.8. Gravimetric Measurements of Water Sorption and Moisture Sorption. The water sorption measurements of materials were carried out at 85 °C, by immersion of dry rectangular samples into deionized water in a water bath. The moisture sorption test was conducted in an environmental chamber maintained at 85 °C and 85% RH. All the samples were prepared in dimensions of 20 mm × 20 mm × 0.9 mm, and

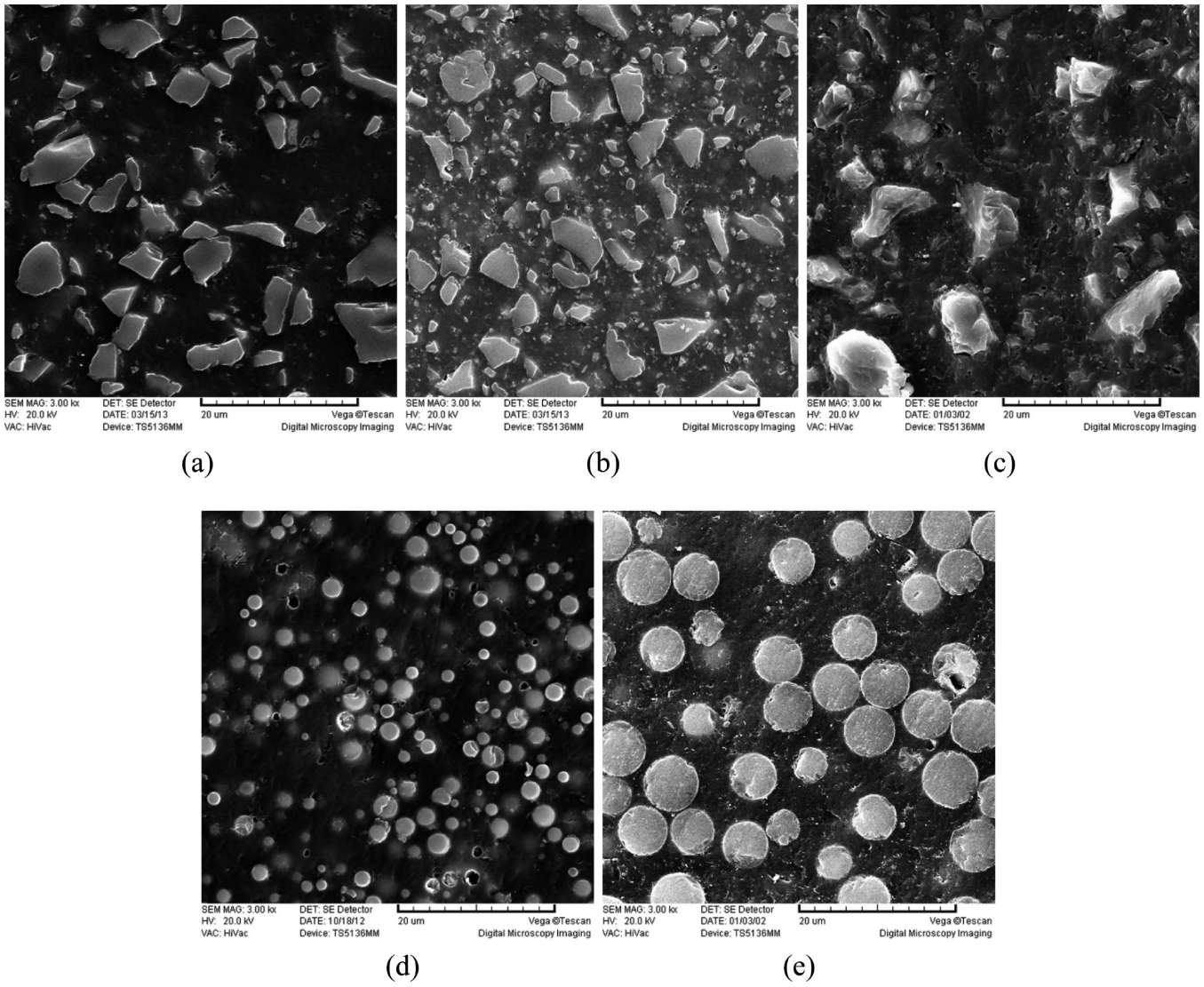

Figure 2. SEM photographs of polished surfaces of cured epoxy packaging materials incorporated with five kinds of fillers: (a) quartz; (b) fused silica; (c) cristobalite; (d) spherical silica; (e) spherical silicone powder.

five specimens of the same component were studied for each sample to get the average value of sorption. Prior to the sorption experiments, all samples were thoroughly washed and then dried in a vacuum oven until a constant dry weight was attained. At appropriate intervals, the samples were removed, wiped down, and quickly weighed on a TG332A microbalance (accuracy, 0.01 mg).

2.2.9. UV Resistance and Thermal Stability. Thermal aging was carried out at 150 °C in a circulating air oven, and UV aging was performed in a UV-203 type UV aging oven, manufactured by Shenzhen Huanghui Co. Ltd. (Shenzhen City, China), at room temperature and in atmosphere. The wavelength of the UV light was 365 nm, and the radiation intensity at the resin surface was 360 mW cm^{-2}. The optical transparency of each sample was obtained in a wavelength range between 300 and 800 nm using a Perkin-Elmer Lambda 35 ultravioletvisible spectrophotometer.

3. RESULTS AND DISCUSSION

3.1. Curing, Thermal, And Optical Properties of the Epoxy Packaging Materials. *3.1.1. Composite Structure.* The filler powders used in this work were characterized by SEM as they were mixed into the resin. Figure 1 shows the variety of filler structures. The spherical silica and spherical silicone powder consist of a spherical structure, while quartz, fused silica, and cristobalite are irregular in shape. The particle size observed in these five fillers is in the range from 2 to 10 μm.

Figure 2 shows the SEM photographs for the polished surfaces of cured epoxy packaging materials incorporated with different fillers. As the mixing procedure changed little the conformation of the micrometer-sized fillers, the size and distribution of the fillers in the composites were almost kept the same as those in the powder. These photographs show a uniform distribution of the particles in the whole volume for all the filled composites.

3.1.2. Curing Behavior. The curing reaction of epoxy resins with anhydride hardeners catalyzed by amine, phosphonium, or metal catalysts is well described in the literature.[38−40] The epoxy groups and anhydride add to each other in an anionic (or cationic sometimes[39]) chain growth mode to form a three-dimensional thermosetting material.

Figure 3 shows the DSC thermograms for filled and unfilled epoxies. The thermal analysis at a heating rate of 10 °C/min was carried out in the temperature range of 20−300 °C. The DSC data, including the onset temperatures and the peak temperatures, are summarized in Table 2. The measured values of the enthalpy (ΔH_r) of the reaction which have been normalized with

dx.doi.org/10.1021/am402035r | ACS Appl. Mater. Interfaces 2013, 5, 8968−8981

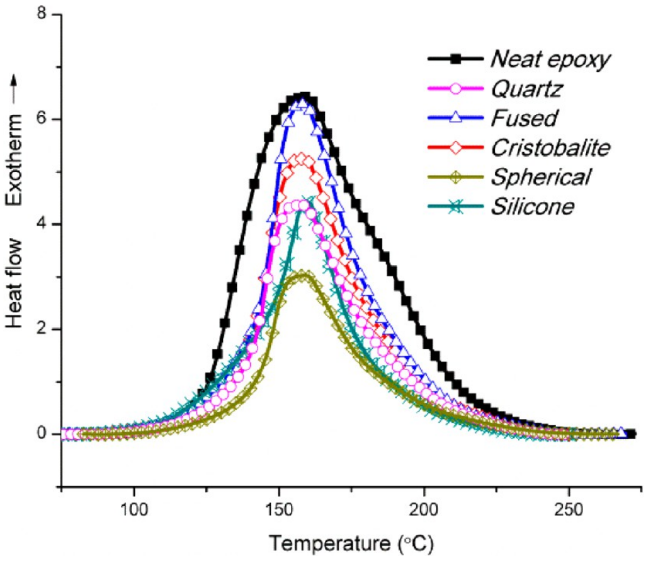

Figure 3. Dynamic curing study of the filled and unfilled epoxies at a heating rate of 10 °C/min by DSC.

respect to the amount of the epoxy resins are also reported in Table 2.

Table 2. Onset, Peak Temperature, and Enthalpy of the Filled and Unfilled Epoxies Obtained by DSC at a Heating Rate of 10 °C/min

systems	neat epoxy	quartz	fused	cristobalite	spherical	silicone
T_{onset} (°C)	123	137	139	137	140	139
T_{peak} (°C)	160	157	159	159	159	160
ΔH_r (kJ/mol)	104	104	106	106	104	102

It could be found that the curing onset temperatures (T_{onset}) are shifted to a higher temperature in the presence of the fillers, while the T_{onset} values of these filled systems appear very close to each other. This could be explained by the addition of the fillers which caused an increase in the viscosity of the system and lowered the concentration of epoxy groups, thus resulting in an increase of the curing onset temperatures due to the drop of the activity of epoxy. Meanwhile, among the filled systems, these retarding effects of the different fillers turned out to be similar by showing the very close values of T_{onset}. The values of ΔH_r kept almost unchanged with the incorporation of the fillers except for *silicone*, indicating that all the four inorganic fillers have little effect on the curing conversion of the composites, while the organic silica filler, *silicone*, would lead a decrease in the curing conversion. It could be also observed that the peak temperature remained nearly constant with the loading of the fillers, which suggested that the fillers show little differences with each other on the reactivity of epoxy composites. In addition, it could be observed that the broadness of curing curves shown in Figure 3 varies among the filled systems. Since the producing procedures, as well as their purities, are quite different for these fillers, which may affect the surface properties of the filler, such as pH values, hydroxyl contents, etc., as a result, their influence on the curing reactions of the blends is unexpected as reported in the literature.[41]

3.1.3. Glass Transition and Thermal Stability. The glass transition temperatures (T_g) of filled and unfilled epoxies were determined on DSC curves as shown in Figure 4, and the values

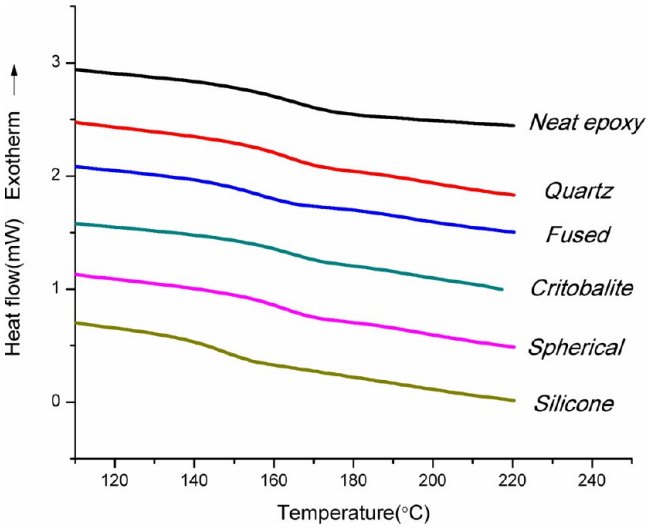

Figure 4. DSC heating curves of filled and unfilled epoxies recorded at a heating rate of 10 °C/min.

are summarized in Table 3. The result showed that the T_g values of *quartz*, *fused*, *cristobalite*, and *spherical* were very close to that

Table 3. Thermal Stability Parameters Calculated from the TGA Curves

systems	neat epoxy	quartz	fused	cristobalite	spherical	silicone
T_{d5} (°C)[a]	355	356	357	350	359	343
char residual at 800 °C (wt %)	1.0	43.0	42.2	43.2	44.1	42.2
T_g (°C)	164	163	155	164	162	147

[a]Temperature at 5% weight loss.

of *neat epoxy*, while *silicone* shows a 10% decrement on T_g values, suggesting a decrease in thermal stability of this system. Figure 5 shows the typical TGA thermograms of the filled and unfilled systems, and the analyzed data are collected in Table 3. Compared to *neat epoxy*, the temperatures at 5% weight loss were essentially the same, while char residuals at 800 °C of ca.

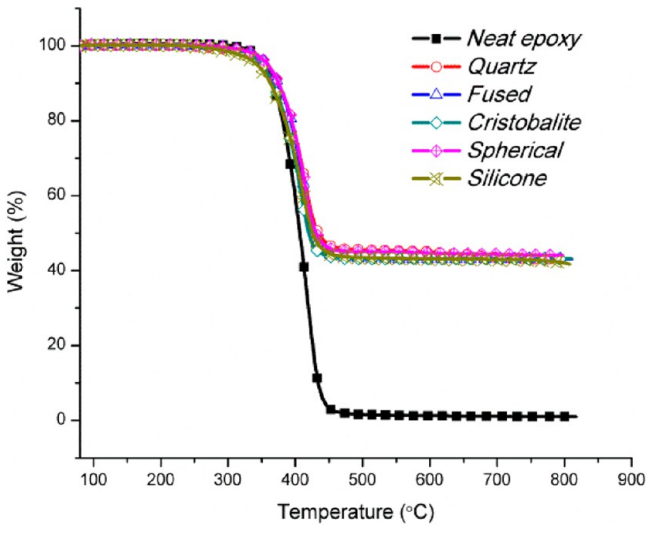

Figure 5. TGA thermographs of filled and unfilled epoxies.

dx.doi.org/10.1021/am402035r | ACS Appl. Mater. Interfaces 2013, 5, 8968−8981

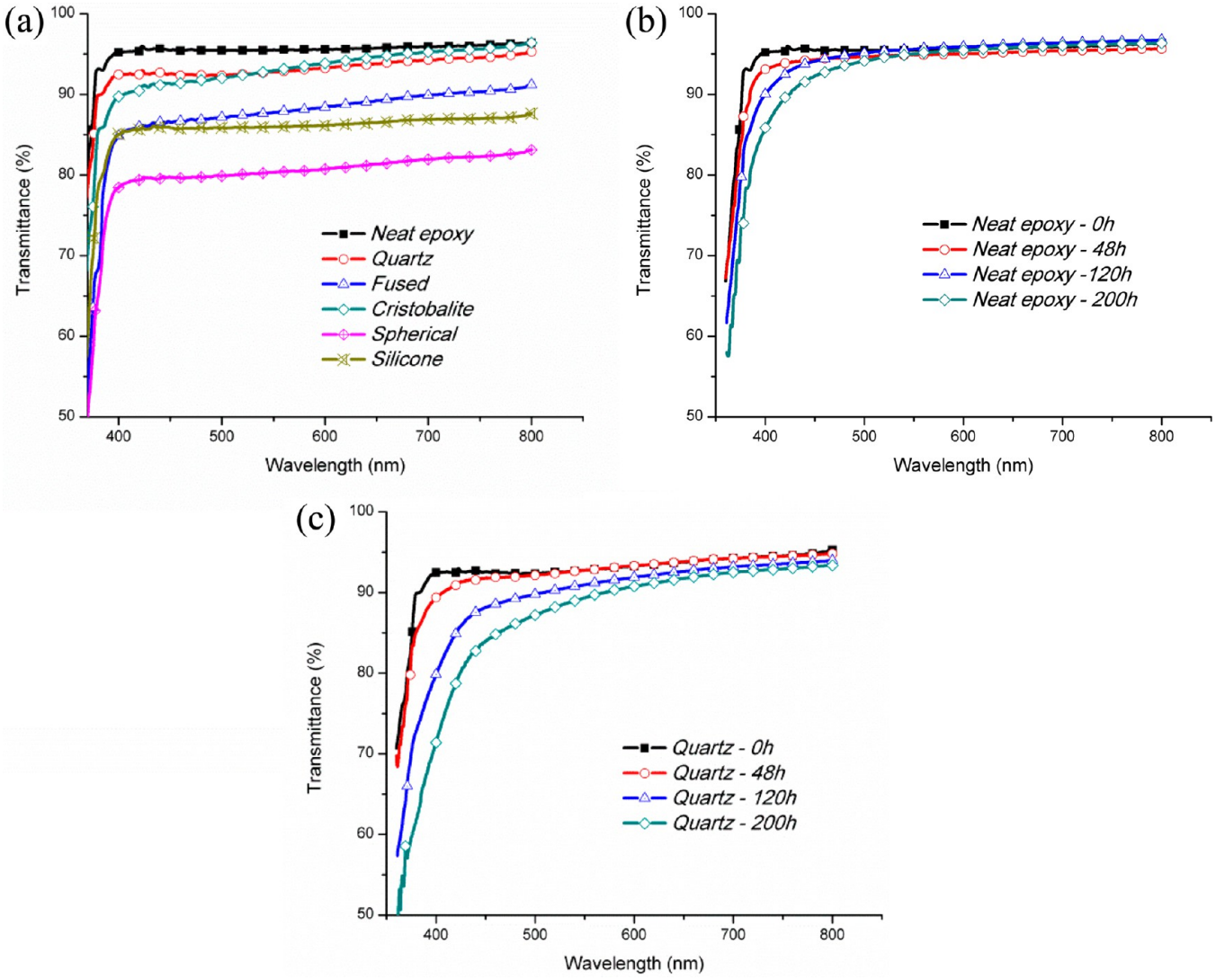

Figure 6. Optical transmittance versus wavelength for filled and unfilled epoxies before thermal aging (a) and the aging behaviors for *neat epoxy* (b) and *quartz* (c), respectively.

40% also coincided well with the solid contents of fillers incorporated into the composites; i.e., the addition of fillers showed few effects on the thermal decomposition of the epoxy packaging materials.

3.1.4. Optical Properties and Thermal and UV Stability. As the refractive index of fillers is different from that of neat epoxy, refraction as well as reflection takes place during light transmitting through the opaque composites. From the point of view of light transmittance of material, the filled composites show lower values than *neat epoxy* as shown in Figure 6 and Figure 7, in which the *neat epoxy* exhibits the highest transmittance than any other system with fillers, suggesting the best transparent appearance it has.

We choose *quartz* as the representative of the filled systems, and its aging behaviors as well as that of the *neat epoxy* are shown in Figure 6 and Figure 7. It could be observed that the decrease of the transmittance in the UV-blue region (ca. 455−390 nm) was accelerated with the addition of the filler powders, which meant that the filled composites would adsorb more blue light and display more yellowing.

The degree of discoloration could be characterized by the increase in yellow index (YI) during thermal and UV aging (Figure 8). YI is represented by the following equation

$$\mathrm{YI} = 100 \times (T_{620} - T_{470})/T_{520} \quad (2)$$

where T_{620}, T_{470}, and T_{520} are the transmittances of the sample at 620, 470, and 520 nm, which correspond to the wavelengths of the three emitting lights (red, green, and blue) of the LED devices in our study.

From Figure 8, it can be found that *neat epoxy* shows the lowest degree of discoloration with the least increase in YI, while among the filled epoxies, the YI values of *quartz* and *cristobalite* are relatively lower both in thermal and UV aging, which suggests a better resistance to discoloration of these two systems. The yellowing of the epoxy formulations was aggravated by the addition of fillers, perhaps partly due to the increase of reflection caused by enlarged differences between epoxy resin and fillers in refractive index.

3.2. Performance and Reliability of LED Devices. For LED devices, the luminous intensity and its stability with thermal/moisture aging are mostly concerned as the main aspect of performance study, while in another aspect, the reliability

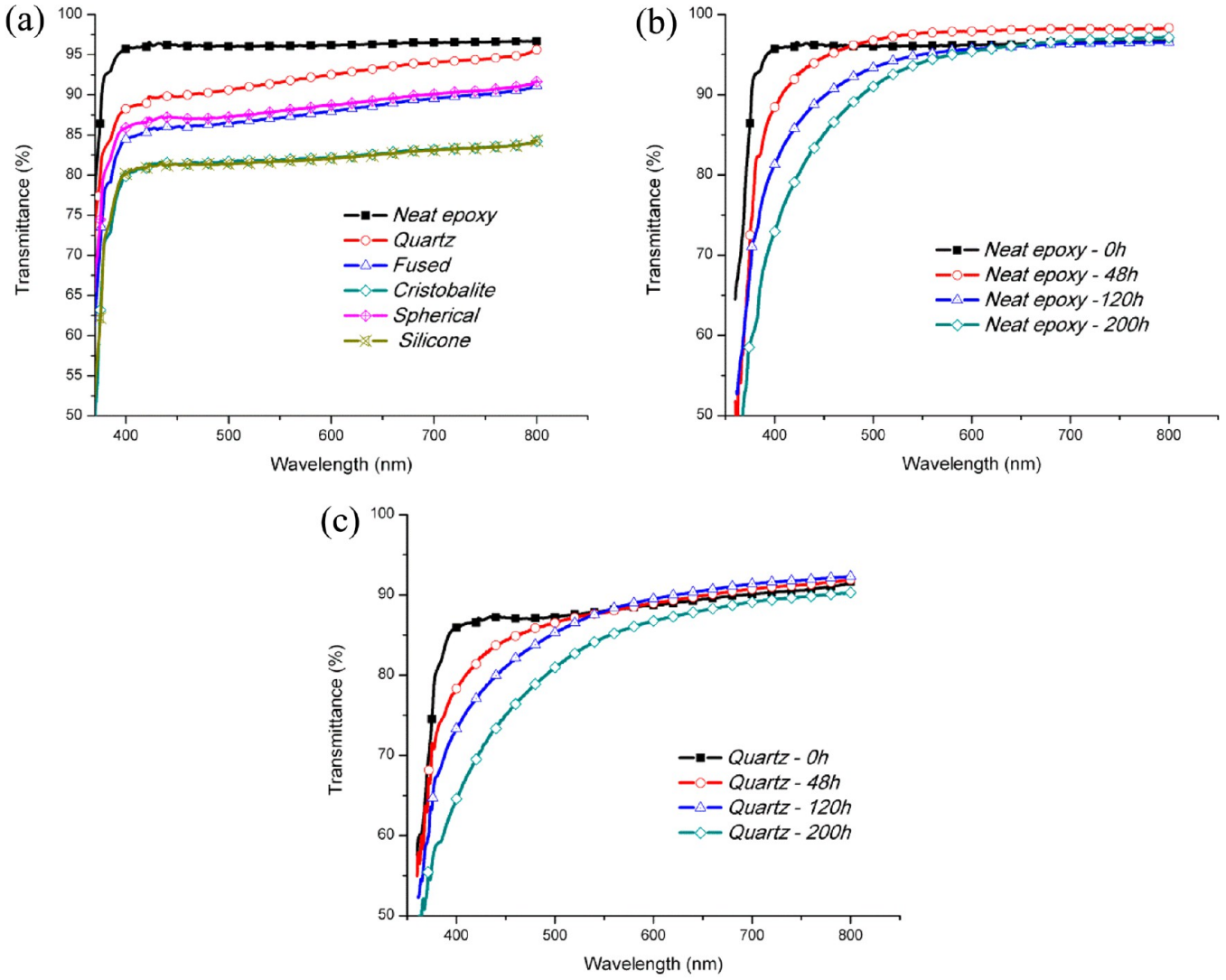

Figure 7. Optical transmittance versus wavelength for filled and unfilled epoxies before UV aging (a) and the aging behaviors for *neat epoxy* (b) and *quartz* (c), respectively.

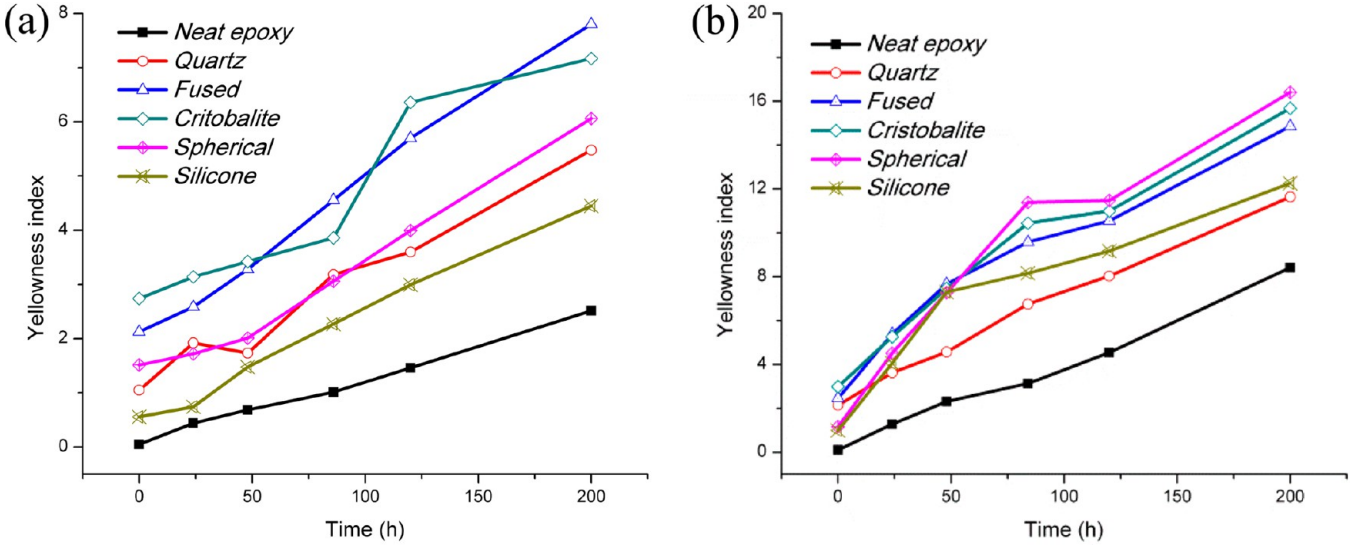

Figure 8. Change in YI for filled and unfilled epoxies during thermal aging (a) and UV aging (b), respectively.

Table 4. Luminous Intensity (mcd) of LED Devices Packaged with Filled and Unfilled Epoxies

light (wavelength)	neat epoxy	quartz	fused	cristobalite	spherical	silicone
red (618.1−619.7 nm)	548.8 ± 34.7	551.5 ± 44.5	578.6 ± 24.5	552.3 ± 32.5	556.8 ± 48.7	462.6 ± 31.9
green (522.0−523.5 nm)	1053.6 ± 48.3	1080.6 ± 56.6	1069.8 ± 48.7	1075.4 ± 57.7	1101.7 ± 58.4	964 ± 77.5
blue (467.4−468.6 nm)	141.8 ± 4.6	153.7 ± 7.6	149.3 ± 3.4	151.6 ± 9.3	157.3 ± 8.6	136.2 ± 12.8

determines the operation life of devices, which has not been well studied until now.

3.2.1. Luminous Intensity and Luminous Flux. From the light transmittance study of the filled and unfilled materials, it seemed that the introduction of fillers might deteriorate the luminous intensity and luminous flux of LED devices. However, the luminous intensity test of LED devices of filled and unfilled packaging materials gave a completely different result as shown in Table 4. The luminous intensity was tested by randomly selecting 100 pieces of surface mount type LEDs for each kind of packaging material encapsulated system. As one can find in Table 4, except *silicone*, all the other four filler added systems show higher luminous intensity than *neat epoxy*; meanwhile, systems with these four silica type fillers show quite limited differences. A similar tendency of filler effect was observed in the luminous flux test as that in the luminous intensity test.

This phenomenon overturns the UV−vis test results of the epoxy packaging materials, in which transparent *neat epoxy* showed much higher light transmittance than the other five packaging materials with fillers. In other words, this result also disagrees with the common sense of transparency for LED packaging materials.

This kind of difference between packaging materials and packaged devices in light transmittance may come from the following reasons. For epoxy materials during UV−vis testing, part of incident light has been reflected back because the refractive index of fillers is different from that of epoxy resin; as a result, the transmission light of materials with fillers is lower than *neat epoxy*, while the UV−vis test of samples has a great difference from that for packaged LED devices, in which the LED chips are buried into the epoxy packaging materials. Most of the light reflected in the resin−filler interface still emits from the LED due to the Ag layer (with very low refractive index of 0.2) reflecting all light out. As high purity inorganic silica fillers have higher light transmittance for visible light than epoxy resins, the addition of fillers lowers the percentage of light being absorbed by epoxy resins. As a result, LEDs packaged with silica filler added materials show higher luminous intensity and flux.

The above experimental results were further demonstrated by hygrothermal aging of the LED devices in 85 °C and 85% RH environment for 1500 h. Figure 9 shows the luminous flux change of LED devices encapsulated with different packaging materials. As the value of blue light changed most while those of red and green varied a little (especially the luminous flux of red light kept unchanged for filled systems), Figure 9 only listed the tendency of blue light with aging time.

The hygrothermal aging led to quite similar results of luminous flux change as that of initial value change of luminous intensity and flux for LED devices. Again, *silicone* showed the worst performance. Comparing with *neat epoxy* packaged LEDs, the four kinds of silica-added LEDs showed much better performance as the luminous flux kept ca. 90% of the initial value, while that of *neat epoxy* only reserved 78% after 1500 h aging; i.e., all the four inorganic silica-type fillers could improve the performance of LED devices even after long-term hygrothermal aging.

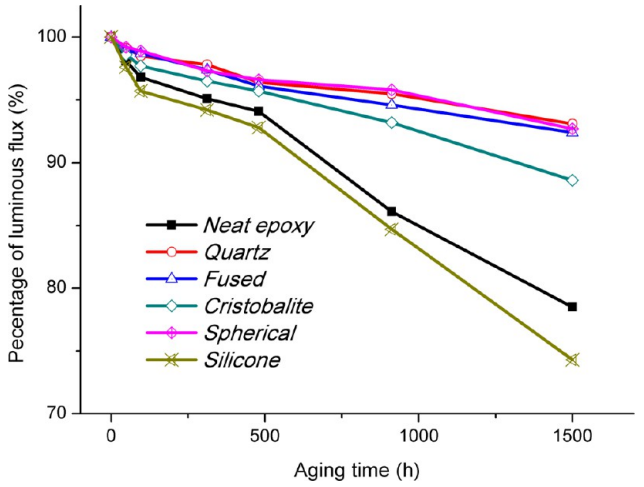

Figure 9. Blue light luminous flux change of LED devices encapsulated with filled and unfilled epoxies during hygrothermal aging at 85 °C and 85% RH environment.

3.2.2. Reliability Test and Luminance Change. Untill now, no standard reliability test method for LED devices has been well established, while most of the aging tests are simply on the basis of thermal aging or UV aging for packaging materials.[4−9,42]

In this work, we have applied the moisture/reflow sensitive level 1 test based on IPC/JEDEC J-STD-020 as the test standard for LED devices, while the luminance change during this test was identified as a kind of aging result.

Table 5 shows the reliability test results based on a modified moisture/reflow sensitive level 1 test procedure. As one can see, LED devices encapsulated with various packaging materials showed great differences during the reflow, PCT, and T/C process. Without any filler, ca. 42% of LEDs failed during 200 rounds of T/C after reflow encapsulated with *neat epoxy*, while the *quartz* packaged system passed 1000 rounds of T/C and PCT with 0% failure. The LED devices encapsulated with *fused* and *spherical* showed almost similar results, and *cristobalite* was somewhat worse than the other three inorganic silica-filled systems. The *silicone* showed even worse performance than *neat epoxy* during the reflow test but somehow better during T/C tests.

Table 6 shows the luminance change during the reliability test, which indicates a similar tendency as that of an accelerated hygrothermal test (Figure 10). Again, the addition of inorganic fillers improved the stability of LEDs during reliability tests, while *silicone* deteriorated the performance of LEDs. As one can see, the system of *quartz* showed the best performance in both the reliability test and aging test, while *fused* and *spherical* were a little worse.

The luminance of LED devices with inorganic fillers showed reversed performance compared to the materials tested by UV−vis. The most possible reason is that aging and reliability tests amplified the refractive index difference between epoxy resin and fillers; as a result, more incident light is reflected during the UV−

Table 5. Reliability Test Results of SMD Type LED Devices Packaged with Filled and Unfilled Epoxies

test item	neat epoxy	quartz	fused	cristobalite	spherical	silicone
−65−150 °C, 5T/C	200/200[a]	200/200	200/200	200/200	200/200	200/200
85 °C, 85% RH, 168 h	200/200	200/200	200/200	200/200	200/200	200/200
reflow profile 3 rounds	200/200	200/200	200/200	200/200	200/200	194/200
PCT	134/200	200/200	200/200	178/200	200/200	156/200
−65−150 °C, 200T/C	115/200	200/200	200/200	185/200	200/200	173/200
−65−150 °C, 500T/C	0/200	200/200	195/200	133/200	193/200	137/200
−65−150 °C, 1000T/C	0/200	200/200	178/200	112/200	182/200	104/200

[a]Pass/test pieces.

Table 6. Luminous flux (blue light) change during reliability test of SMD type LED devices packaged with filled and unfilled epoxies

test item	neat epoxy	quartz	fused	cristobalite	spherical	silicone
−65−150 °C, 5T/C	99.2%	99.7%	99.6%	99.3%	99.8%	98.7%
85 °C, 85% RH, 168 h	101.2%	104.3%	104.4%	101.5%	104.1%	94.6%
reflow profile 3 rounds	96.4%	102.2%	101.8%	98.4%	101.7%	93.4%
−65−150 °C, 200T/C	94.5%	99.7%	98.6%	96.5%	99.4%	89.8%
−65−150 °C, 500T/C	--	99.4%	97.9%	92.8%	98.7%	86.2%
−65−150 °C, 1000T/C	--	99.1%	97.1%	92.7%	98.1%	83.9%

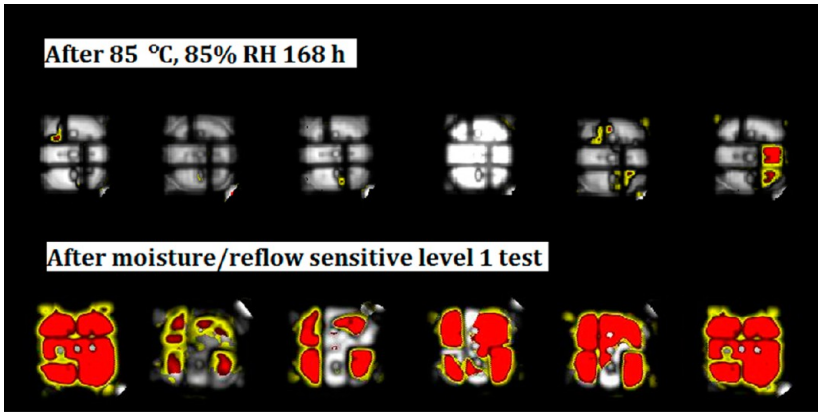

Figure 10. C-SAM (scanning acoustic micrograph) images of LED devices showing the extent of delamination at the interface during reliability tests. The samples from left to right are *neat epoxy*, *quartz*, *fused*, *cristobalite*, *spherical*, and *silicone*.

vis test for packaging materials, which makes the materials with fillers seem to be worse than *neat epoxy* during aging tests.

Figure 10 shows the C-SAM image at the die pad interface after moisture sorption and IR reflow. It was manifested that the inorganic fillers had a positive effect on the adhesion to the die pad substrate, which showed varying amounts of delamination originating at the corners of the die, while complete delamination took place in both *neat epoxy* and *silicone* after IR reflow. After 168 h of water sorption, LEDs with neat epoxy and inorganic fillers have no crack at the interface, as indicated by the contrast in the images, whereas some part of delamination could be observed in the *silicone*; i.e., the filler of silicone gives a negative effect on the moisture sorption of packaging materials.

Figure 11(a) shows a photo of an encapsulated LED device as an example. The cross section of the packaged LED devices was studied by SEM for further analysis of the site of delamination. For *neat epoxy* and *silicone* systems, extensive delamination on the lead frame area had been observed (not shown in this article). The SEM micrographs of *fused* and *spherical* systems were somewhat similar to C-SAM tests, while for *quartz* systems, no delamination could be found in the interface either between packaging materials and LED chips or between packaging materials and the Ag/Cu layer (Figure 11 b,c); however, the delamination observed by C-SAM was demonstrated to be the crack of polyphthalamide frame (Figure 11c), which needs to be improved in the future.

3.3. Analysis of the Relationship between Reliability and Properties of Epoxy Materials. To better understand the effects of fillers on the performance and reliability of LED devices, moisture sensitivity and physical properties of the packaging materials were measured.

3.3.1. Water and Moisture Sorption. Thermal stress as well as moisture absorbed by the packages is the main cause for the delamination in electronic packaging materials. Moisture diffuses into the package, makes the package swell, and reduces interfacial adhesion strength. The mismatching coefficients of moisture expansion (CMEs) will induce hygromechanical stress in the package[43] and thus enlarge the mismatching CTE in LED packages and internal stress when the package is heated in the reflow soldering process. From this point, the water sorption behavior of packaging materials has a great impact on the reliability of LEDs.

The gravimetric measurements of water sorption (in 85 °C hot water) and moisture sorption (85 °C/85RH) for comparison are presented in Figure 12(a) and (b), respectively. Two parameters

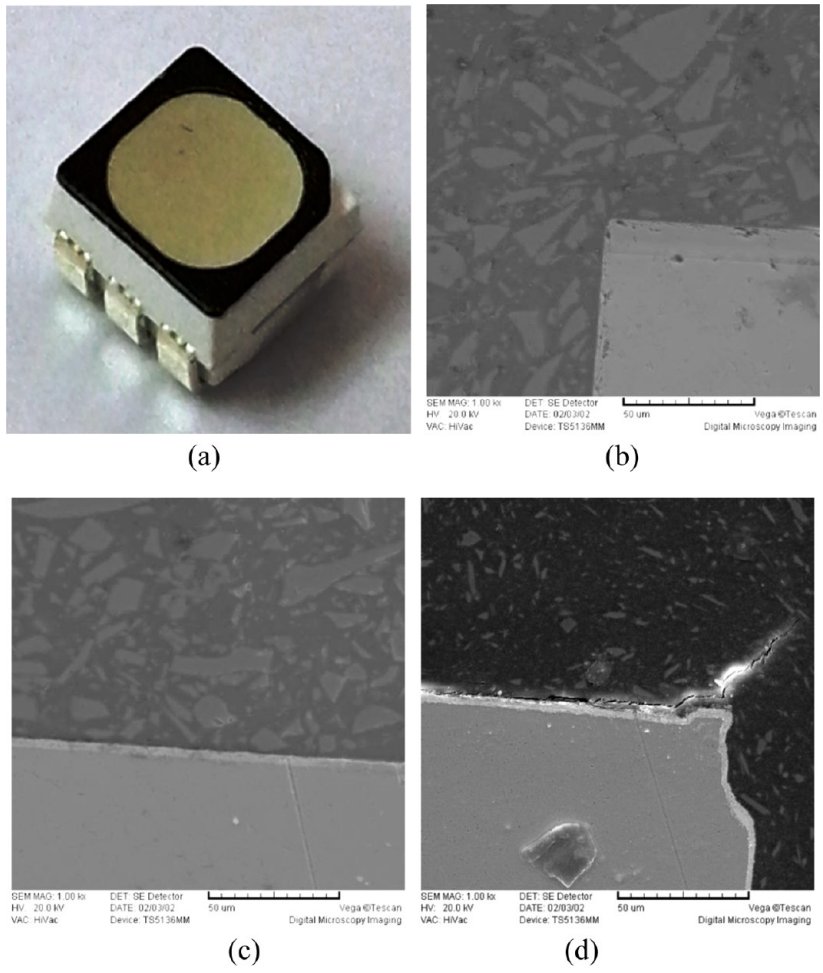

Figure 11. Encapsulated LED device and SEM micrographs of the interfaces after Level-1 test. (a) A sample of encapsulated LED device. (b) *Quartz* packaging materials and LED chip. (c) *Quartz* packaging materials and Ag/Cu layer. (d) Polyphthalamide frame and Ag/Cu layer.

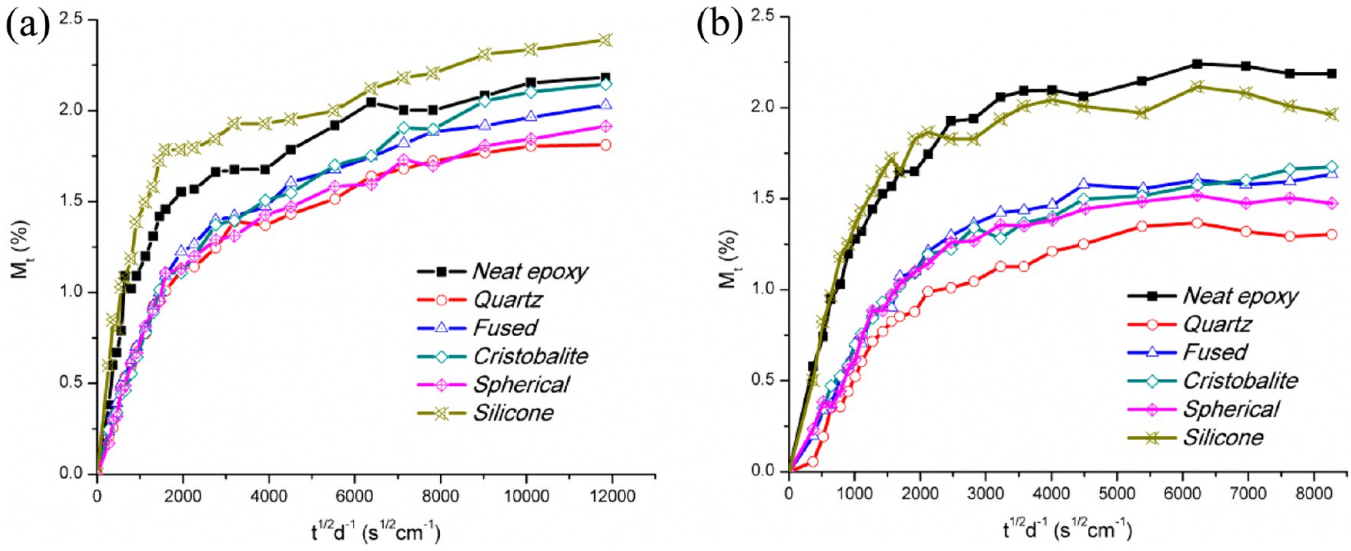

Figure 12. Gravimetric results of water (a) and moisture (b) diffusion into different epoxy systems.

as equilibrium water sorption and diffusion coefficient are closely related to the properties of packaging materials.

Generally, the behavior of sorption curves in epoxy can be modeled by Fick's second law, with the diffusion coefficients fulfilling the following equation[44]

$$\frac{M}{M_{\max}} = 1 - \sum_{n=0}^{\infty} \frac{8}{(2n+1)^2\pi^2} \exp\left[\frac{-D(2n+1)^2\pi^2 t}{4L^2}\right] \quad (3)$$

dx.doi.org/10.1021/am402035r | ACS Appl. Mater. Interfaces 2013, 5, 8968−8981

Table 7. Calculated Results from Gravimetric Measurements

systems		neat epoxy	quartz	fused	cristobalite	spherical	silicone
water sorption	$^{a}M_{max}$	2.18	1.81	2.03	2.15	1.91	2.39
	^{b}D	6.33	2.67	2.10	1.87	2.44	7.34
moisture sorption	$^{a}M_{max}$	2.20	1.30	1.59	1.63	1.49	2.04
	^{b}D	6.92	4.07	3.73	3.46	3.47	10.1

[a]The unit of equilibrium water content is % by weight. [b]The unit of diffusion coefficient is 10^{-8} s^{-1} cm^2.

Table 8. Comparisons of the Coefficients of Thermal Expansion (CTE) and T_g Obtained From the TMA Experiment

systems		neat epoxy	quartz	fused	cristobalite	spherical	silicone
α (ppm K^{-1})	below T_g	73	57	48	59	49	79
	above T_g	140	135	131	145	126	126
T_g (°C)		166	164	162	163	165	156

where D is the diffusion coefficient; L is the thickness of the specimen; and M_{max} is the equilibrium value of the diffusing water at infinite time.

When the values of M_t/M_{max} are lower than 0.5, eq 3 can be simplified as below

$$\frac{M}{M_{max}} = \left(\frac{4}{L\sqrt{\pi}}\sqrt{D}\right)\sqrt{t} \quad (4)$$

and the diffusion coefficient D can be calculated by plotting M/M_{max} as a function of the square root of time divided by the thickness of the sample.

The water sorption (uptake at time t, M_t) of the sample was achieved as below

$$M_t = [(W_t - W_0)/W_t] \times 100 \quad (5)$$

where W_0 is the weight of the dry specimen and W_t is the weight of the wet specimen at time t.

Diffusion coefficients (D) acquired by curve fitting and equilibrium water contents (M_{max}) gained from Figure 12 for both water sorption and moisture sorption are presented in Table 7.

In Figure 12, except for *neat epoxy*, the M_{max} value of each system obtained in water sorption was higher than the corresponding one in moisture sorption measurement due to the more severe conditions in the water sorption test. Except for *silicone*, the values of equilibrium water content (M_{max}) for inorganic silica-filled systems in both water sorption and moisture sorption tests were lower than that of *neat epoxy*. The M_{max} value of *silicone* in the water sorption test was a little higher than that of *neat epoxy*, while the value in the moisture sorption test was very close to that of *neat epoxy*. Among the filled systems, *quartz* gave the best performance, of which the value of M_{max} decreased about 17% compared with *neat epoxy* in the water sorption test and 40% in the moisture sorption test. As the bulk fillers absorb little water, there are mainly two parts, i.e., the resin matrix and interface, which absorb most of the water. In our previous study,[45,46] we have found that M_{max} is mainly determined by the polarity and the free volume of the system. Compared to *neat epoxy*, *silicone* has higher free volume, while the interface between epoxy and silicone powder also absorbs water, which results in a higher M_{max} in the sorption test.

The diffusion behaviors of six epoxy formulations in both tests showed a similar tendency, which followed the sequence *silicone* > *neat epoxy* > the other silica-filled epoxies, while the slopes of moisture sorption curves were a little smaller than those of the water sorption test. Besides *silicone*, the diffusion coefficient was lowered by the addition of filler powders, and the value for *cristobalite* was lowest, which was about 70% less than that of *neat epoxy* in the water sorption test and 50% in the moisture sorption test. Meanwhile, it is worth noting that the higher D values of moisture sorption calculated according to eq 5, which has also been observed in the work of Mondragon et al.,[47] may be attributed to the lower M_{max} obtained in the moisture sorption test.

As the delamination during IR reflow (popcorn) is caused by the vapor pressure of water, lower water content would clearly favor the performance during solder reflow. Therefore, both the water sorption and moisture sorption results definitely indicated the best performance of the *quartz* system, which exhibited the lowest equilibrium water content and relatively lower water diffusion rate, while *silicone* was just the opposite, which showed higher values of diffusion rate and equilibrium water content.

3.3.2. Effects of Fillers on CTE. CTE mismatch of dissimilar materials is identified as the primary factor which leads to die paddle and glue delamination at the corner of the molding compound and lead frame, where the epoxy glue and chip are highly stressed. Table 8 shows the results of CTE measurements for epoxy composites. It could be observed that except for the system *silicone* CTE values below T_g decreased with the loading of the silica fillers, showing a reduction ranging from 20% to 34% as compared to the *neat epoxy*. In general, it is well-known that the CTE of polymer materials is decreased by the addition of silica particles.[10,48]

However, in the case of *silicone*, CTE gave a higher value in comparison with *neat epoxy*. As the CTE of silicone (polymethylsilsesquioxane) is higher than that of silica, the CTE of *silicone* is therefore higher than those of other filled materials. When temperature reached above T_g, except for the system *cristobalite*, the other filled formulations showed reduced CTE values, while it is worth noting that the reduced extent was less than that below T_g.

From these results, we suppose that the free volume in filled systems might be larger than that of the unfilled systems and be more rapidly increased with an increase in the ambient temperature. When temperature is below T_g, the magnitude of increase in free volume is relatively small, and thus its effect on CTE is small too. Therefore, the CTE values could be reduced a lot by the incorporation of silica fillers. However, with the temperature increase, the free volume increases rapidly, and its impact on CTE is becoming larger, thus leading to a lesser extent of CTE reduction above T_g. Furthermore, when this effect of the free volume exceeds that of the silica fillers, the CTE values of the composites will be increased, whereas compared to other fillers, silicones exhibit a relatively better interaction with the matrix due

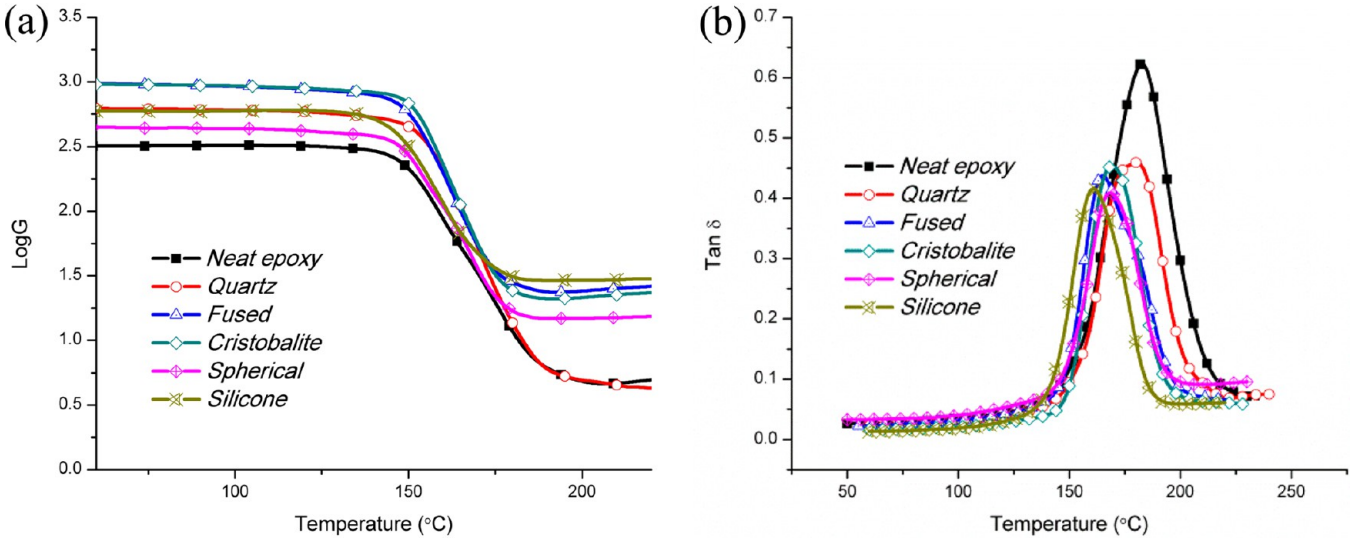

Figure 13. Dynamic mechanical study of filled and unfilled epoxies. (a) Logarithm of storage modulus versus temperature and (b) tan δ versus temperature.

Table 9. Thermal and Mechanical Properties of Filled and Unfilled Epoxies

samples	neat epoxy	quartz	fused	cristobalite	spherical	silicone
$^{a}T_g$ (°C)	183	180	165	169	168	161
$^{b}T_g$ (°C)	148	153	148	151	147	142
$^{c}E_r$ (MPa)	4.66 ± 0.28	2.12 ± 0.05	26.2 ± 1.03	23.4 ± 0.92	15.3 ± 0.17	30.1 ± 0.56
hardness (Shore D)	79	80	81	80	79	78

$^{a}T_g$ determined as the peak temperature of the tan δ. $^{b}T_g$ determined as the onset temperature of the storage modulus. ^{c}The storage modulus at 260 °C.

to the organic groups attached to the filler surface. This would constrict the expansion of the resin matrix above T_g due to the quick growth of free volume, and as a result, the CTE value of *silicone* above T_g is lower than those of other systems.

On the whole, the formulations of *spherical*, *quartz*, and *fused* gave the best performance among the filled systems, which exhibited the reduced CTE values both below and above T_g. The T_g values obtained from TMA experiment are also summarized in Table 8 and corresponded well to those determined from the DSC test.

3.3.3. Internal Stress Analysis. Generally, internal stress during T/C, especially thermal stress during solder reflow, between two material interfaces can be calculated by[49]

$$\sigma = \int E(T)a(T)\mathrm{d}T \tag{6}$$

where E is the Young's modulus; α is the coefficient of thermal expansion; and T is temperature.

As the T_g of all these packaging materials is above 150 °C and the curing temperature is 150 °C, at which temperature the thermal stress can be deemed as zero, we can then simplify the above equation as:

$$\mathrm{SI}_{T/C} = E_{T/C} \times (150 - T) \times \alpha_1 \tag{7}$$

$$\mathrm{SI}_{260} = E_{260} \times (260 - T_g) \times \alpha_2 + E_{25} \times (T_g - 150) \times \alpha_1 \tag{8}$$

where SI is stress index; E, T_g, α_1, and α_2 are the Young's modulus, glass transition temperature, and CTE below and above T_g; $\mathrm{SI}_{T/C}$ is the internal stress during the T/C process; and SI_{260} is that during IR reflow.

From eq 8, it can be found that the thermal stress during IR reflow is closely related to the Young's modulus and CTE above T_g. As the T_g of packaging materials is quite close to 150 °C, SI_{260} therefore could be simplified as $110E_{260}\alpha_2$.

The Young's modulus can be measured by DMA for both values above and below T_g. Figure 13 shows the dynamic mechanical spectra for the filled and unfilled epoxies, and the values of modulus and T_g measured from it are listed in Table 9. The hardnesses of the filled and unfilled epoxies are also summarized in Table 9. As shown in Figure 13(b), the tan δ versus temperature curves of the composites are affected by the addition of the fillers. For all the materials only one single T_g relaxation could be identified, which reflected the formation of homogeneous systems in filled epoxy resins. In Table 9, it is shown that all filler incorporated systems display the α transition (glass transition) peaks shifting to lower temperatures, which was different from the tendency observed in DSC and TMA tests. However, the T_g values determined from the onset temperature of the storage modulus corresponded well to the results from DSC and TMA, where all filled systems exhibited a T_g very close to that of *neat resin* except for *silicone* which exhibited a 4% decrease. We believe that the different changing trends of T_g values between *silicone* and other filled systems was caused by the different surface properties between organic silicone fillers and inorganic silica fillers. Among the filled systems, only *silicone* showed the dropping down of T_g and thus displayed the worst thermal stability compared to other formulations. Table 9 also shows the changes of Shore D hardness for filled and unfilled epoxies. It could be observed that the hardness values for

dx.doi.org/10.1021/am402035r | ACS Appl. Mater. Interfaces 2013, 5, 8968−8981

different formulations were very close to each other, which may imply that the addition of fillers shows a limited effect on the mechanical strength.

As can be seen in Figure 13(a), the Young's modulus is greatly increased with the presence of the filler below the glass temperature, which could be explained by the reinforcing effect of the filler. The modulus showed a dependence on the type of particles, which should result from the different dispersion qualities and interfacial properties in the filler incorporated systems.

For LED packaging materials, a low modulus at high temperature above T_g can minimize the thermal stress during IR reflow. A representative modulus at reflow temperature was taken at 260 °C, and the values of filled and unfilled systems are summarized in Table 9, in which the system of *quartz* exhibits the lowest storage modulus, showing a decrease of 54% compared with *neat epoxy*. Combined with its low CTE, the *quartz* system had the lowest thermal stress among all the systems. Even more, the decreased equilibrium water sorption and diffusion coefficients of *quartz* could effectively diminish the popcorn during IR reflow. Consequently, no delamination took place in the interface of packaging materials and lead frame, and thus *quartz* possessed the best performance and reliability.

4. CONCLUSION

A set of evaluated method have been established successfully to characterize the performance and reliability of LED devices, which is based on a combination of moisture, IR reflow, thermal cycling, and luminous test during the test procedure. We have also put forward that the UV−vis test is not a reliable method for the light transmittance study of the packaging materials used in LEDs.

Five kinds of filler, including four kinds of inorganic silicas and silicone, were incorporated into epoxies as LED packaging materials to compare the performance of encapsulated LED devices. Except for *silicone*, all the filled systems showed lower equilibrium water sorption content and smaller water diffusion coefficient in both the water sorption test and moisture sorption test compared with *neat epoxy*. Quartz gave the best performance with the value of M_{max} decreasing by about 17% in the water sorption test compared to *neat epoxy* and 40% in the moisture sorption test, while *cristobalite* exhibited the lowest water diffusion coefficient, around 70% less than that of the neat system in the water sorption test and 50% in the moisture sorption test. The CTE values have also been decreased with the addition of filler. A reduction of 20% to 34% in CTE was observed below T_g, while a smaller reduction was obtained above T_g. The system of *quartz*, *fused*, and *spherical* gave the best performance, which exhibited the reduced CTE values both below and above T_g. The UV−vis test showed that the transparency was decreased with the addition of fillers, while the luminous intensity test overturned this result. The glass transition temperature changed little for all the filled systems, except *silicone* which showed a 4% decrease from the DMA test. The results of TGA indicated that the addition of fillers showed few effects on the thermal stability of the epoxy packaging materials.

It showed that the system of *quartz* exhibited the best performance in both the reliability test and aging test, and no delamination could be found in the interface either between packaging materials and LED chips or between packaging materials and the Ag/Cu layer, which could be well explained by the balanced properties of *quartz*: the lowest water sorption content, relatively lower water diffusion coefficient, decreased CTE values, good UV and thermal stability, and especially lowest storage modulus at reflow temperature.

AUTHOR INFORMATION

Corresponding Author

*Tel.: +86-21-65642865. Fax: +86-21-65640293. E-mail: yfyu@fudan.edu.cn.

Notes

The authors declare no competing financial interest.

ACKNOWLEDGMENTS

This research work was supported by the National Natural Science Foundation of China (Grant 21274031).

REFERENCES

(1) Chang, M. H.; Das, D.; Varde, P. V.; Pecht, M. *Microelectron. Reliab.* **2012**, *52*, 762−782.
(2) Gao, N.; Liu, W.; Ma, S.; Tang, C.; Yan, Z. *J. Polym. Res.* **2012**, *19*, 9923.
(3) Huang, J. C.; Chu, Y.-P.; Wei, M.; Deanin, R. D. *Adv. Polym. Technol.* **2004**, *23*, 298−306.
(4) Lin, Y. C.; Tran, N.; Zhou, Y.; He, Y.; Shi, F. G. Materials challenges and solutions for the packaging of high power LEDs. *Microsystems, Packaging, Assembly Conference Taiwan*, Taipei, 2006; IEEE.
(5) Tsuchida, S.; Osaka, M. Epoxy resin composition for sealing photo-semiconductor element and photo-semiconductor device sealed with the epoxy resin composition. U.S. Patent 5,985,954, November 16, 1999.
(6) Chu, Y. P. Epoxy resin systems for light-emitting diode. *Master*, University of Massachusetts Lowell, 2003.
(7) Yasumasa, M. UV-resistant epoxy resin, and light emitting diode or wavelength conversion element sealed by using the epoxy resin. JP 2003-012896, January 15, 2003.
(8) Lin, Y. C. Materials for optoelectronic device packaging/manufacturing. *Ph.D.*, University of California, Irvine, 2007.
(9) Zhou, Y. Study of liquid transparent encapsulants for the packaging of light emitting diode and other optoelectronic devices. *Ph.D*, University of California, Irvine,, 2008.
(10) Wong, C. P.; Wong, M. M. *IEEE Trans. Compon. Packag. Technol.* **1999**, *22*, 21−25.
(11) Pecht, M. G.; Govind, A. *IEEE Trans. Compon., Packag., Manuf. Technol., Part C.* **1997**, *20*, 207−212.
(12) Groothuis, S. K.; Heinen, K. G.; Rimpillo, L. Effects of mold compound material properties on solder reflow package cracking. *Reliability Physics Symposium, 1995. 33rd Annual Proceedings*, IEEE International, 1995; IEEE.
(13) Hu, J.; Yang, L.; Whan Shin, M. *Microelectron. J.* **2007**, *38*, 157−163.
(14) Lantz, L.; Hwang, S.; Pecht, M. *Microelectron. Reliab.* **2002**, *42*, 1163−1170.
(15) Ma, X.; Jansen, K. M. B.; Ernst, L. J.; van Driel, W. D.; van der Sluis, O.; Zhang, G. Q. *Microelectron. Reliab.* **2007**, *47*, 1685−1689.
(16) Maggana, C.; Pissis, P. *J. Polym. Sci., Part B: Polym. Phys.* **1999**, *37*, 1165−1182.
(17) Fan, J. J.; Yung, K. C.; Michael, P. *IEEE Trans. Device Mater. Reliab.* **2011**, *11*, 407−416.
(18) Olmos, D.; Martínez, F.; González-Gaitano, G.; González-Benito. *Eur. Polym. J.* **2011**, *47*, 1495−1502.
(19) Brian, J. T.; Barry, B.; Christy, M. Underfills, Adhesives and Coatings in Electronics Assemblies. In *Electronic Materials and Processes Handbook*, 3rd ed.; Charles, A. H., Ed.; McGraw-Hill Professional: New York, 2004; Vol. *9*, pp 573−633.
(20) Gerard. K. An Introduction to Plastic Packaging. *The simulation of thermomechanically induced stress in plastic encapsulated IC packages*; Kluwer Academic Publishers: Dordrecht, 1999; Vol. *1*, pp 1−12.

(21) Kinjo, N.; Ogata, M.; Nishi, K.; Kaneda, A. Epoxy molding compounds as encapsulation materials for microelectronic devices. In *Speciality Polymers/Polymer Physics*; Berry, G. C., Matyjaszewski, K., Eds.; Advances in Polymer Science 88; Springer Berlin Heidelberg: Berlin, 1989; pp 1−48.
(22) Kanaji, K.; Mizuike, K.; Nishiguchi, T. High performance liquid epoxy encapsulant for advanced semiconductor package. *Electronic Packaging Technology Conference, 1997. Proceedings of the 1997 1st*, 1997; IEEE.
(23) Fujii, A.; Andoh, M.; Yamamoto, I.; Ibuki, H.; Uchida, K.; Yoshizumi, A. New epoxy molding compounds for SMT with pre-plated lead-frame system. *Electronics Manufacturing Technology Symposium, 1998. Twenty-Third IEEE/CPMT*, 1998; IEEE.
(24) Yorkgitis, E. M.; Eiss, N. S.; Tran, C.; Wilkes, G. L.; McGrath, J. E. *Adv. Polym. Sci.* **1985**, *72*, 79−109.
(25) Nakamura, Y.; Tabata, H.; Suzuki, H.; Iko, K.; Okubo, M.; Matsumoto, T. *J. Appl. Polym. Sci.* **1986**, *32*, 4865−4871.
(26) Ho, T. H.; Wang, C. S. *Eur. Polym. J.* **2001**, *37*, 267−274.
(27) Tuller, H. W.; Nussbaum, R. W. Encapsulant compositions based on anhydride-hardened epoxy resins. U.S. Patent 4,042,550, August 16, 1977.
(28) Wong, C.; McBride, R. *IEEE Trans. Adv. Packag.* **1993**, *16*, 868−875.
(29) Müller, R.; Heckmann, K.; Habermann, M.; Paul, T.; Stratmann, M. *J. Adhes.* **2000**, *72*, 65−83.
(30) Suzuki, O.; Kawamoto, S. Development of Low Stress No-Flow Underfill for Flip-Chip Application. *Electronic Components and Technology Conference*, 2005; IEEE.
(31) Du, X.; Xie, G.; Tan, W.; Qin, S.; Cheng, X. Stress Reduction of Epoxy Molding Compound and Its Effect on Delamination. *High Density packaging and Microsystem Integration, 2007. HDP'07. International Symposium on*, 2007; IEEE.
(32) Mont, F. W.; Kim, J. K.; Schubert, M. F.; Schubert, E. F.; Siegel, R. W. *J. Appl. Phys.* **2008**, *103*, 083120.
(33) Chung, P. T.; Yang, C. T.; Wang, S. H.; Chen, C. W.; Chiang, A. S. T.; Liu, C. Y. *Mater. Chem. Phys.* **2012**, *136*, 868−876.
(34) Kazuhiro, F.; Shinya, O. Epoxy Resin Composition for Optical-Semiconductor Element Encapsulation and Optical-Semiconductor Device Using the Same. U.S. Patent 2011/0272829, November 10, 2011.
(35) Ota, S.; Fuke, K.; Goto, C.; Ito, H.; Taniguchi, T.; Yoshida, K.; Gunji, M.; Takuwa, S. Epoxy resin composition for optical semiconductor element encapsulation and optical semiconductor device using the same. U.S. Patent 7,986,050, July 26, 2011.
(36) Rubinsztajn, M. I.; Rubinsztajn, S. Composition comprising silicone epoxy resin, hydroxyl compound, anhydride and curing catalyst. U.S. Patent 6,632,892, October 14, 2003.
(37) Yeager, G. W.; Rubinsztajn, M. I. Composition of cycloaliphatic epoxy resin, anhydride curing agent and boron catalyst. U.S. Patent 6,617,400, September 9, 2003.
(38) Huang, J. C.; Chu, Y. P.; Wei, M.; Deanin, R. D. *Adv. Polym. Technol.* **2004**, *23*, 298−306.
(39) Blank, W. J.; He, Z. A.; Picci, M. *J. Coat. Technol.* **2002**, *74*, 33−41.
(40) Morita, Y. *J. Appl. Polym. Sci.* **2009**, *114*, 2301−2306.
(41) Akatsuka, M.; Takezawa, Y.; Amagi, S. *Polymer* **2001**, *42*, 3003−3007.
(42) Trevisanello, L.; Meneghini, M.; Mura, G.; Vanzi, M.; Pavesi, M.; Meneghesso, G.; Zanoni, E. *IEEE Trans. Device Mater. Reliab.* **2008**, *8*, 304−311.
(43) Wong, E.; Chan, K.; Rajoo, R.; Lim, T. The mechanics and impact of hygroscopic swelling of polymeric materials in electronic packaging. *Electronic Components & Technology Conference, 2000. 2000 Proceedings. 50th*, 2000; IEEE.
(44) Park, G. S. *Diffusion in Polymers*; Academic Press: New York, 1968.
(45) Li, L.; Yu, Y. F.; Wu, Q. L.; Zhan, G. Z.; Li, S. J. *Corros. Sci.* **2009**, *51*, 3000−3006.
(46) Li, L.; Yu, Y. F.; Su, H. H.; Zhan, G. Z.; Li, S. J.; Wu, P. Y. *Appl. Spectrosc.* **2010**, *64*, 458−465.
(47) Imaz, J. J.; Rodriguez, J. L.; Rubio, A.; Mondragon, I. *J. Mater. Sci. Lett.* **1991**, *10*, 662−665.
(48) Teh, P. L.; Jaafar, M.; Akil, H. M.; Seetharamu, K. N.; Wagiman, A. N. R.; Beh, K. S. *Polym. Adv. Technol.* **2008**, *19*, 308−315.
(49) Lin, L. L.; Ho, T. H.; Wang, C. S. *Polymer* **1997**, *38*, 1997−2003.